Anisotropic oxidation of crystallites of vanadyl pyrophosphate

Gaku Koyano, Fumihiro Yamaguchi, Toshio Okuhara [1] and Makoto Misono

Department of Applied Chemistry, Graduate School of Engineering, The University of Tokyo, Bunkyo-ku, Tokyo 113, Japan

Received 7 May 1996; accepted 16 July 1996

Anisotropic oxidation of crystallites of vanadyl pyrophosphate ($(VO)_2P_2O_7$) has been demonstrated by Raman spectroscopy with samples having different microstructures. Oxidation of these samples by O_2 produced X_1 phase, α- and β-$VOPO_4$ phases. The relative peak intensity of the X_1 phase to the other phases correlated well with the ratio of the (100) plane to the side planes (surface area-basis). This correlation showed that the (100) plane was oxidized to X_1 phase and the side planes to α- and β-$VOPO_4$. For example, thin plate-like $(VO)_2P_2O_7$, of which the (100) fraction is 98%, was oxidized almost exclusively to X_1 phase. But when it was fractured into small plates to increase the side planes and then oxidized, α- and β-$VOPO_4$ were detected in addition to the X_1 phase. These results are consistent with our previous conclusion that the (100) plane of $(VO)_2P_2O_7$ is selective, but side planes are non-selective for catalytic oxidation of *n*-butane.

Keywords: vanadyl pyrophosphate; Raman spectroscopy; anisotropic oxidation; X_1 phase; α-$VOPO_4$; β-$VOPO_4$; *n*-butane oxidation

1. Introduction

Vanadyl pyrophosphate, $(VO)_2P_2O_7$, is the main component of an industrial catalyst for the production of maleic anhydride (abbreviated as MA) by selective oxidation of *n*-butane [1–3]. There are different proposals for the active phase of this catalyst; for example, the single crystalline phase of $(VO)_2P_2O_7$ [4–6], a biphasic catalyst consisting of $(VO)_2P_2O_7$ and γ-$VOPO_4$ [7,8], and a phosphorus-rich phase [9,10]. A variety of crystallites of $(VO)_2P_2O_7$ having different shape or morphology showed different activity and selectivity for *n*-butane oxidation. $(VO)_2P_2O_7$ having rose-like crystallites has been reported to be highly active [6,11,12]. Horowitz et al. further reported that incorporation of tetraethyl orthosilicate into $(VO)_2P_2O_7$ increased exposure of the (100) plane and in consequence the catalytic activities increased [13]. Since the (100) plane is the dominant surface of this rose-like $(VO)_2P_2O_7$, the active crystal plane of $(VO)_2P_2O_7$ is thought to be (100), on which V^{4+}–O–V^{4+}(=O) pair sites are located [6,13–16]. Ziolkowski et al. have proposed on the basis of a crystallographic model that the (100) plane of $(VO)_2P_2O_7$ is efficient for the selective oxidation of *n*-butane [14]. Igarashi et al. concluded that the difference in the selectivity for different samples of $(VO)_2P_2O_7$ at higher conversions is due to the difference in activity for oxidation of MA [15]. Okuhara et al. have demonstrated by using large plate-like crystallites of $(VO)_2P_2O_7$ that the (100) plane is selective for the formation of MA, while side planes ((001), (021), etc.) are non-selective [16].

Raman spectroscopy has been proven to be useful to study redox processes and surface phases of VPO catalysts [17–19]. Volta and co-workers claimed that a V^{5+} phase, γ-$VOPO_4$, formed on the surface is active for the selective oxidation [17,18]. We showed that X_1 phase is involved in the surface redox process of $(VO)_2P_2O_7$ [19].

Here we wish to report the anisotropic oxidation, that is, upon oxidation, the X_1 phase is preferentially formed on the (100) plane and α- and β-$VOPO_4$ on side planes of $(VO)_2P_2O_7$. The anisotropy is closely related to the different activity and selectivity observed for the planes of the crystallites [16].

2. Experimental

Three kinds of precursors, all being vanadium hydrogen phosphate hemihydrate ($VOHPO_4 \cdot 0.5H_2O$) (P-1; from an aqueous solution, P-3; organic solvent method, P-4; by the reduction of $VOPO_4 \cdot 2H_2O$ with 2-butanol), were prepared according to the literature [15]. Vanadyl pyrophosphate ($(VO)_2P_2O_7$, C-1, C-3 and C-4, were obtained by the treatment of P-1, P-3 and P-4, respectively, at 823 K in an N_2 flow for 5 h [15]. The crystallites of C-4 were fractured into smaller crystallites (abbreviated as C-4(fr)) by the method as described previously [16]. The structures of C-1, C-3, and C-4 were confirmed to be $(VO)_2P_2O_7$ by using XRD [15].

According to SEM, C-1 consists of thick plate-like crystallites, C-3 rose petal-like, and C-4 thin plate-like crystallites, as reported previously [15]. After C-4 was fractured five times, the width decreased to about 1 μm, and new side planes were created as reported before [16].

[1] Present address: Graduate School of Environmental Earth Science, Hokkaido University, Sapporo 060, Japan.

Table 1
Microstructure of vanadium phosphorus oxides

	BET surface area ($m^2\ g^{-1}$)	Thickness along [100] [a] (nm)	Width of (100) plane [b] (nm)	Fraction of (100) plane [c] (surface area base) (%)
C-1	10	100	300	60
C-3	78	8	1000	98
C-4	13	40	5000	98
C-4(fr) [d]	15	40	1000	91
X_1 phase	28	–	–	–
β-$VOPO_4$	3	–	–	–

[a] Estimated from XRD line width.
[b] Determined from SEM.
[c] Calculated from the shape and size of the crystallites.
[d] After the fracture.

The thickness of the crystallite along [100] was estimated from the line width of XRD ($2\theta = 22.8°$) and the width (size) was determined by SEM (table 1) [15]. The fraction of (100) plane was calculated from the width and the thickness of the crystallites assuming the shape of the crystallites as square prisms.

Bulk X_1 phase (28 $m^2\ g^{-1}$) was synthesized from NH_4HVPO_6, as described previously [4]. This phase is most likely the same as δ-$VOPO_4$ reported by Bordes [8] and the β'' phase reported by Matsuura [20]. α-$VOPO_4$ (6.6 $m^2\ g^{-1}$) and β-$VOPO_4$ (3.2 $m^2\ g^{-1}$) were prepared according to the literature [4].

Oxidation of $(VO)_2P_2O_7$ was performed in an O_2 flow for 2 h at 733–773 K, after the $(VO)_2P_2O_7$ was pretreated in He at 773 K for 1 h. The oxidation state of catalyst is expressed in two ways; x in $VPO_{4.5+x}$ and the number of V^{5+} surface layers (NL), which was estimated as described previously [19]. Raman spectra were recorded with a laser Raman spectrometer (Jasco Corporation, NR-1800) using the 514.4 nm line from an Ar ion laser (NEC GLS3261J) [19].

Catalytic oxidation of MA was performed in a conventional flow reactor of Pyrex tube (inside diameter: 10 mm) at 713 K using a gas mixture of 1.5% MA, 17% O_2, and N_2 balance (flow rate: 20 $cm^3\ min^{-1}$) [15], after the catalysts (100 mg) were treated in N_2 (60 $cm^3\ min^{-1}$) at 773 K for 1 h.

3. Results and discussion

Fig. 1 shows the changes in Raman spectra of $(VO)_2P_2O_7$ upon the oxygen treatment at 753 K. It was observed that C-1 and C-3 (before the O_2 treatment; spectra a and c) gave the same spectra as reported in the literature [21]; the main peak was located at 923 cm^{-1}, which is assigned to ν(P–O–P) [21]. When C-3 was oxidized at 753 K ($x = 0.097$, NL = 1.9), new peaks were detected at 937, 1020, and 1090 cm^{-1} (fig. 1b), which are close to those of X_1 phase (fig. 1e), and were different from those of α-$VOPO_4$ (930 and 1040 cm^{-1}, fig. 1f) or β-$VOPO_4$ (896, 987, and 1072 cm^{-1}, fig. 1g). On the other hand, oxidized C-1 (753 K, $x = 0.044$, NL = 4.4) showed peaks at 896, 987, 1040, and 1072 cm^{-1}, together with the peaks of $(VO)_2P_2O_7$ and X_1 phase at 923, 937, 1020, and 1090 cm^{-1} (fig. 1d). The new peaks (896, 987, and 1072 cm^{-1}) are attributed to β-$VOPO_4$. The small peak at 1040 cm^{-1} is due to α-$VOPO_4$ [17]. The spectra of α- and β-$VOPO_4$ are shown in figs. 1f and 1g. Thus, it is evident that C-3 was oxidized to X_1 phase and C-1 to a

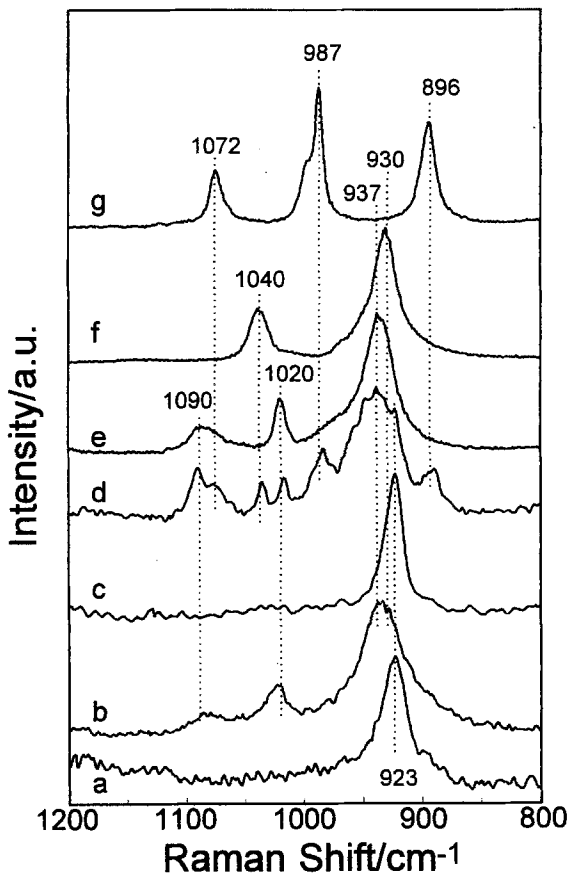

Fig. 1. Raman spectra of (a) $(VO)_2P_2O_7$ (C-3) before oxidation, (b) C-3 after oxidation at 753 K ($x = 0.097$, NL = 1.9), (c) $(VO)_2P_2O_7$(C-1), (d) C-1 after oxidation at 753 K ($x = 0.044$, NL = 4.4), (e) X_1 phase, (f) α-$VOPO_4$, and (g) β-$VOPO_4$.

mixture of X_1 phase, α- and β-$VOPO_4$. Although Raman spectroscopy contains bulk information, and the amount of X_1 phase is about 1/10 that of $(VO)_2P_2O_7$ phase, the peak intensity of X_1 phase was comparable to that of $(VO)_2P_2O_7$ phase. This is due to the difference in the Raman sensitivity between X_1 phase and $(VO)_2P_2O_7$; the sensitivity of the peak (937 cm^{-1}) due to X_1 phase is about 10 times greater than that (923 cm^{-1}) of $(VO)_2P_2O_7$ [19].

The distinct difference in oxidation as described above may be attributed to the difference in crystal habits. C-3 and C-1 have rose petal-like particles and thick plate-like particles, respectively [15]. Since the fraction (on the basis of the surface area) of the (100) plane (basal plane) is 98 and 60% for C-3 and C-1, respectively (table 1), the different oxidized phases may be explained by anisotropic oxidation of the crystal planes, i.e., the (100) plane is oxidized to X_1 phase and the side planes (e.g. (021), (012), and (001)) to α- and β-$VOPO_4$. The intensity ratio of the peak at 937 cm^{-1} (X_1 phase) to the sum of the two peaks at 930 cm^{-1} (α-$VOPO_4$) was about 1.7 for oxidized C-1 (fig. 1d), where these peaks are due to P–O stretching [5,17]. This value was close to the ratio of the surface area of the (100) plane to that of side planes of C-1, that is, 1.5. Since the sensitivities of these Raman peaks, 937 cm^{-1} (X_1 phase), 930 cm^{-1} (α-$VOPO_4$), and 987 cm^{-1} (β-$VOPO_4$), were observed to be similar by comparing with the main peak (498 cm^{-1}) of cystine (pellet) which was used for an external standard, the relative intensities of these peaks correspond to the relative amounts of these phases present in the sample.

To confirm the anisotropic oxidation, the oxidation was carried out for a sample of which the surface area of the side planes was intentionally increased. The thin plate-like $(VO)_2P_2O_7$ (C-4) was fractured into small plates (denoted by C-4(fr)) as described previously [16]. Raman spectra of C-4 and C-4(fr) are shown in fig. 2. C-4 and C-4(fr) before the oxidation showed the same spectra as $(VO)_2P_2O_7$ (figs. 2a and c) [21]. When C–4 was oxidized at 753 K ($x = 0.038$, NL = 4.5), a small peak at 1020 cm^{-1} due to X_1 phase appeared (fig. 2b), while the main peak of X_1 phase (937 cm^{-1}) was not evident due to the overlap with the peak (923 cm^{-1}) of $(VO)_2P_2O_7$. The peak at 1090 cm^{-1} corresponding to X_1 phase was too small to be observed. On the other hand, for C-4(fr), new weak peaks at 1040 cm^{-1}, due to α-$VOPO_4$, and 896, 987, and 1072 cm^{-1}, which are assignable to β-$VOPO_4$, were detected after the oxidation (fig. 2d). This result indicates that the side planes newly formed were oxidized mainly to α- and β-$VOPO_4$.

If one considers that a redox mechanism is generally accepted for the oxidation of *n*-butane, and that the surface of $(VO)_2P_2O_7$ was partially oxidized during the reaction [19,22,23], the results of the present study are explained consistently with the anisotropic catalysis

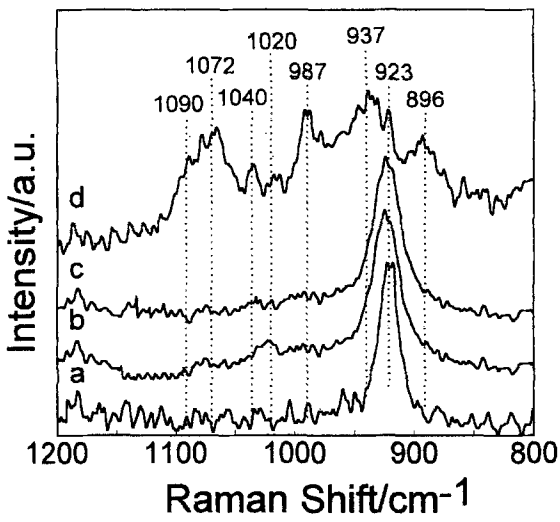

Fig. 2. Raman spectra of (a) $(VO)_2P_2O_7$ (C-4) before oxidation, (b) C-4 after oxidation at 753 K ($x = 0.038$, NL = 4.5), (c) C-4(fr) before oxidation, and (d) C-4(fr) after oxidation at 753 K ($x = 0.063$, NL = 6.5).

of $(VO)_2P_2O_7$ crystallites as reported previously [6,13,14,16]. The (100) plane of $(VO)_2P_2O_7$ has been considered to be selective for the catalytic oxidation of *n*-butane, while the side planes were non-selective [6,13,14,16]. It has further been shown that α- and β-$VOPO_4$ were much less selective for catalytic *n*-butane oxidation than the X_1 phase [4,24], and that stoichiometric reduction of the surface X_1 phase with *n*-butane gave MA with a higher selectivity than that for β-$VOPO_4$ [19]. Thus the X_1 phase is reasonably thought to have more favorable surface than α- or β-$VOPO_4$ for the selective oxidation of *n*-butane.

One reason for the low selectivity of β-$VOPO_4$ is secondary oxidation of MA [15]. As shown in table 1, when C-4 was fractured the size of the crystallites decreased from 5000 to 1000 nm. As the change in the surface area upon the fracture was small (table 1), the fracture most probably brought about the increase in the surface area of the side planes, keeping nearly constant the surface area of the basal plane (100), as was discussed previously [16]. It was found that the reaction rate (per unit surface area) for the oxidation of MA increased from 3.8×10^{-6} to 5.3×10^{-6} mol m^2 min^{-1}. This indicates that the side planes are more active in MA oxidation than the (100) plane. Side planes may have partially changed to α- and β-$VOPO_4$ during the oxidation of *n*-butane, resulting in the formation of non-selective surface.

In conclusion, the anisotropic oxidation of the crystal plane was demonstrated; the (100) plane is oxidized to X_1 phase and side planes to α- and β-$VOPO_4$. X_1 phase on the (100) plane catalyzes selective oxidation and α- and β-$VOPO_4$ formed on the side planes cause non-selective oxidation of *n*-butane and consecutive oxidation of product MA.

References

[1] G. Centi, F. Trifirò, J.R. Ebner and V.M. Franchetti, Chem. Rev. 88 (1988) 55.
[2] B.K. Hodnett, Catal. Rev. Sci. Eng. 27 (1985) 373.
[3] G. Centi, Catal. Today 16 (1993) 5.
[4] T. Shimoda, T. Okuhara and M. Misono, Bull. Chem. Soc. Jpn. 58 (1985) 2163.
[5] T.P. Moser and G.L. Schrader, J. Catal. 92 (1985) 216.
[6] G. Busca, F. Cavani, G. Centi and F. Trifirò, J. Catal. 99 (1986) 400.
[7] N.H. Batis, H. Batis, A. Ghorbel, J.C. Vedrine and J.C. Volta, J. Catal. 128 (1991) 248.
[8] E. Bordes and P. Courtine, J. Chem. Soc. Chem. Commun. (1985) 294.
[9] H. Morishige, J. Tamaki, N. Miura and N. Yamazoe, Chem. Lett. (1990) 1513.
[10] M.T. Sananes, G.J. Hutchings and J.C. Volta, J. Chem. Soc. Chem. Commun. (1995) 243; J. Catal. 154 (1995) 253.
[11] E.C. Milberger, N.J. Bremer and D.E. Dria, US Patent 4333853 (1982).
[12] R.A. Schneider, US Patent 4043943 (1977).
[13] H.S. Horowitz, C.M. Blackstone, A.W. Sleight and G. Teufer, Appl. Catal. 38 (1988) 193.
[14] J. Ziolkowski, E. Bordes, and P. Courtine, J. Catal. 122 (1990) 126; J. Mol. Catal. 84 (1993) 307.
[15] H. Igarashi, K. Tsuji, T. Okuhara and M. Misono, J. Phys. Chem. 97 (1993) 7065.
[16] T. Okuhara, K. Inumaru and M. Misono, *Catalytic Selective Oxidation*, ACS Symp. Ser. 523 (Am. Chem. Soc., Washington, 1993) p. 156;
K. Inumaru, T. Okuhara and M. Misono, Chem. Lett. (1992) 1955.
[17] F.B. Abdelouahab, R. Olier, N. Guilhaume, F. Lefebvre and J.C. Volta, J. Catal. 134 (1992) 151.
[18] G.J. Hutchings, A.D. Chomel, R. Olier and J.C. Volta, Nature 368 (1994) 41.
[19] G. Koyano, T. Okuhara and M. Misono, Catal. Lett. 32 (1995) 205.
[20] I. Matsuura, A. Mori and M. Yamazaki, Chem. Lett. (1987) 1897.
[21] T.P. Moser and G.L. Schrader, J. Catal. 104 (1987) 99.
[22] M.A. Pepera, J.L. Callahan, M.J. Desmond, E.C. Milberger, P.R. Blum and N.J. Bremer, J. Am. Chem. Soc. 107 (1985) 4883.
[23] Y.Z. Lin, M. Forissier, R.P. Sneeden, J.C. Vedrine and J.C. Volta, J. Catal. 145 (1994) 267.
[24] Y.Z. Lin, M. Forissier, R.P. Sneeden, J.C. Vedrine and J.C. Volta, J. Catal. 145 (1994) 256.